Available online at www.sciencedirect.com
ScienceDirect
Journal of Molecular Catalysis A: Chemical 281 (2008) 173–178
JOURNAL OF MOLECULAR CATALYSIS A: CHEMICAL
www.elsevier.com/locate/molcata

Toluene combustion on γ-Al_2O_3–CeO_2 catalysts prepared from boehmite and cerium nitrate

G. Del Angel [a,*], J.M. Padilla [a], I. Cuauhtémoc [a], J. Navarrete [b]

[a] *Universidad Autónoma Metropolitana-Iztapalapa, Departamento de Química, Área de Catálisis, Av. San Rafael Atlixco No. 186, C.P. 09340, AP 55-534, México, D.F., Mexico*
[b] *Instituto Mexicano del Petróleo, Programa de Ingeniería Molecular, México, D.F. 07730, Mexico*

Available online 24 August 2007

Abstract

γ-Al_2O_3–Ce catalysts were obtained by the impregnation of boehmite with cerium nitrate at different Ce contents (1, 5, 10, 20 wt%) and tested in the catalytic combustion of toluene. The catalysts annealed at 650 °C showed a diminution of the BET specific surface areas as a function of the cerium content. At low cerium content, the XRD spectra showed the γ-Al_2O_3 phase, whereas at high cerium content, the γ-Al_2O_3 phase and cerium oxide were observed. A diminution of the Lewis acidity was shown by the FTIR-pyridine absorption spectra. Both Ce^{3+} and Ce^{4+}in variable proportions were observed by XPS. It has been found that the activity for the toluene combustion can be related to the C^{4+}/Ce^{3+} ratio obtained in the various catalysts. The higher the C^{4+}/Ce^{3+} ratio is the higher the toluene combustion activity.

Keywords: Alumina–ceria catalysts; XPS alumina–ceria characterization; Alumina–ceria; Alumina–ceria XRD patterns; Alumina–ceria Lewis acidity; Alumina–ceria toluene combustion

1. Introduction

The catalytic combustion is a convenient way for the pollution control of a wide range of volatile organic compounds (VOCs), such as hydrocarbons, oxygenated organic molecules, halogenated compounds, etc. In particular, aromatic compounds are important environmental pollutants since they are known as carcinogenic agents. The aromatic compounds that are found as atmospheric pollutants come from the evaporation of different sources such as solvents, gasoline; and as byproducts from industrial processes. The aromatic combustion has been mainly focused on the study of the catalytic behavior of supported noble metals such as platinum and palladium on well-known supports such as Al_2O_3, SiO_2, TiO_2, ZrO_2 [1–3]. The combustion activity of noble metals supported on various mixed oxides has also been reported [4,5]. In general, it is accepted that the supported metal is the responsible of the catalytic combustion; and the role of the support is restricted to the heat and metal sintering control. However, in recent papers, it has been reported that metal oxide catalysts such as Al, Cu, Mn, Ti, Ce Zn, etc. [6] or perovskites have shown important catalytic combustion activities [7,8]. The importance of the economical and application feasibilities to use metallic oxides without noble metals has attracted the attention of a large number of scientists in their studies and applications concerning the VOC abatement.

Ceria has the capacity to store and liberate oxygen due to the redox properties of the Ce^{3+}/Ce^{4+} pair which results in a good performance for either the oxidation of CO or the volatile organic compounds combustion [9–11]. However, ceria shows a very low stability under severe conditions at which the VOC oxidation occurs; and as for industrial applications, its stabilization is necessary. Nowadays, the ceria–alumina supported systems constitute one of the most widely used mixed-oxide systems for elimination of pollutants in automobile exhaust gases [12]. However, the catalytic properties of the Al_2O_3–CeO_2 materials for the total oxidation of VOCs have rarely been used without supporting noble metals. In the present work, we focused on the study of Al_2O_3–CeO_2 (1, 5, 10 and 20 wt% Ce) mixed oxides in the toluene combustion. The ceria–alumina mixed oxides were obtained by adding cerium nitrate to alumina boehmite. The method allows better cerium oxide stabilization on the alumina support after calcination. Afterwards, an intensive characterization of the Ce–alumina supports was performed by means of the XRD, FTIR-pyridine adsorption and XPS studies. The catalytic

* Corresponding author.
E-mail address: gdam@xanum.uam.mx (G. Del Angel).

1381-1169/$ – see front matter © 2007 Elsevier B.V. All rights reserved.
doi:10.1016/j.molcata.2007.08.017

oxidative properties of these materials were determined in the toluene combustion in a flow reactor.

2. Experimental

2.1. Catalyst preparation

The γ-Al_2O_3 reference catalyst was obtained by calcination, under air flow (3.6 L h^{-1}) at 650 °C for 4 h, boehmite (Catapal–B CONDEA high purity 99.999%, 26% H_2O, 220 m^2 g^{-1}). The ceria-alumina catalysts were prepared by adding to the boehmite a solution containing $Ce(NO_3)_3{\cdot}6H_2O$ (Strem 99.99%) at the desired Ce content (1, 5, 10 and 20 wt% Ce); and maintained under stirring for 4 h. Afterwards, the solids were dried at 60 °C in a rotary evaporator. The solids were dried at 120 °C for 12 h; and then calcined at 650 °C for 24 h in air flow (3.6 L h^{-1}). For their identification, the samples were labeled as: A for alumina; and ACeX for the cerium–alumina samples, where X indicates the amount of Ce (1, 5, 10 and 20 wt%) contained in the catalyst.

2.2. Specific surface areas

The specific surface areas were determined by nitrogen adsorption in a Quantachrome Multistation Autosorb 3B analyzer. Before performing the adsorption, the calcined supports were outgassed at 400 °C in vacuum (10^{-3} Torr) for 2 h. The specific surface areas were calculated by the BET equation.

2.3. X-ray diffraction analysis

The X-ray diffraction patterns of the supports were obtained to identify the alumina phases in the samples. A SIEMENS-D500 diffraction instrument equipped with a Cu Kα radiation anode and a graphite monochromator in the secondary beam was used. The specimens were prepared by packing the powdery samples into glass holders. The intensity data were measured by step scanning through the 2θ ranges between 2° and 70° with a 2θ step of 0.02°; and a measuring time of 1 s/point. The identification of the phases was carried out by using the corresponding JCPDS cards for the different oxides.

2.4. FTIR-pyridine adsorption

The pyridine adsorption was studied with a Nicolet model 170-SX FTIR spectrophotometer. The powdered samples were pressed until reaching transparency and placed in a Pyrex glass cell equipped with CaF_2 windows. Before performing the pyridine adsorption, the samples were pretreated in vacuum (10^{-3} Torr) at 400 °C for 30 min in order to clean the surface. The samples were then cooled to room temperature and pyridine was introduced by breaking a capillary tube containing the pyridine. After 30 min of pyridine-support adsorption equilibrium, the pyridine excess was removed under vacuum for 10 min; and then the spectra were recorded at various desorption temperatures.

2.5. X-ray photoelectron spectroscopy (XPS)

The XPS analyses were carried out by using a THERMO VG ESCALAB 250 spectrometer equipped with an aluminum anode (energy of 1486.8 eV) and an X-ray system monochromator. The X-ray source was powered at 15 kV and 7.5 mA. In order to correct the effect of charge in the XPS spectra, all the binding energies were referenced to the C 1s line of adventitious carbon at 284.6 eV. The samples were placed on a thin sheet of indium and then analyzed. In order to control the sample charge in all the experiments, an electron flood gun was used. No additional treatment was applied to the samples prior to these measurements.

2.6. Catalytic activity measurements

The toluene combustion in vapor phase was carried out in a conventional continuous flow U-shape glass reactor used in the differential mode at atmospheric pressure. Toluene of 1400 ppm in air was used as reactant in a total flow of 90 mL min^{-1}. The catalyst (0.1 g) was first treated under air flow (90 mL min^{-1}) at 500 °C for 45 min, in order to clean the surface; afterwards, the toluene–air reactant mixture (1400 ppm toluene) was passed through the reactor during 15 min at 500 °C. Then, the temperature was cooled down to 100 °C under the reactant mixture. The combustion reaction was carried out from 100 to 400 °C with a program rate of 1 °C min^{-1}. The conversions were measured during this range of temperature. The pretreatment of the catalysts with the reaction mixture was made to stabilize the catalysts in order to avoid the large fluctuations in activity observed when the reaction was carried out with fresh catalysts [13].

Reactants and products were analyzed by using an on-line gas chromatographer VARIAN 3400 CX equipped with a TCD (thermal conductivity detector) and a FID (flame ionization detector) using a J&W Scientific Megaboro 30 m, with a phase GSQ column that allowed measurements of CO_2 and H_2O concentrations; and a PONA of 50 m columns to follow toluene conversion. The only products, identified and confirmed by a HP-GC-MS 5973 gas chromatographer mass spectrometer, were CO_2 and H_2O.

3. Results and discussion

The preparation method, the addition of cerium nitrate to boehmite, leads to a diminution of the BET specific surface area of the supports calcined at 650 °C: 174, 164, 156, 157 and 128 m^2 g^{-1} for the A, ACe1, ACe5, ACe10 and ACe20 samples, respectively, Fig. 1. The diminution of the specific surface areas was of the order of 6–27% for contents of 1–20 wt% Ce. This drop in the specific surface area increases with the Ce load, showing that the cerium oxide modifies the textural properties of the γ-Al_2O_3. The cerium effect can be seen in the slight shift to larger pore size diameter (Fig. 2).

The effect of cerium on the stability of the calcined alumina at different temperatures is illustrated in Fig. 1. As for the reference alumina, the decay in the specific surface area was more

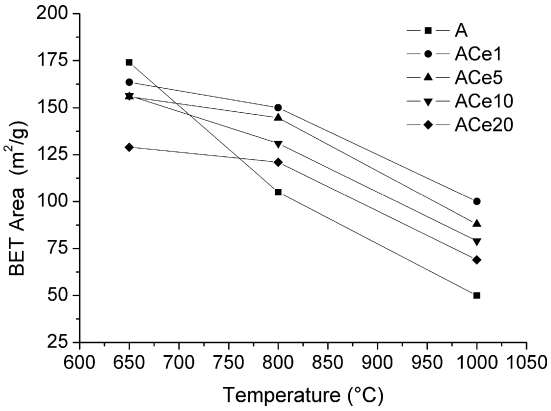

Fig. 1. Specific surface areas for the A, ACe1, ACe5, ACe10 and ACe20 catalysts as functions of the cerium content after thermal treatment at 650, 800, and 1000 °C.

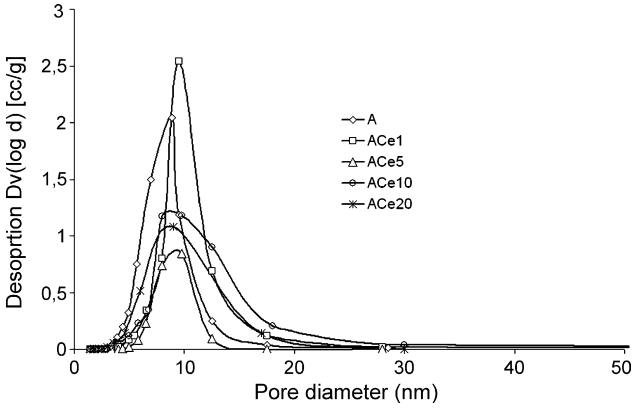

Fig. 2. Pore size diameter distribution as a function of the cerium load.

remarkable than that observed in the cerium–alumina containing supports.

The X-ray diffraction spectra of the samples calcined at 650 °C are shown in Fig. 3. As for the solid with 1.0 wt% Ce, just the peaks corresponding to γ-Al_2O_3 can be observed, suggesting that Ce could be highly dispersed on the γ-Al_2O_3; therefore, the CeO_2 peaks cannot be detected by XRD. At higher Ce wt% content, the peaks assigned to CeO_2 are clearly identified

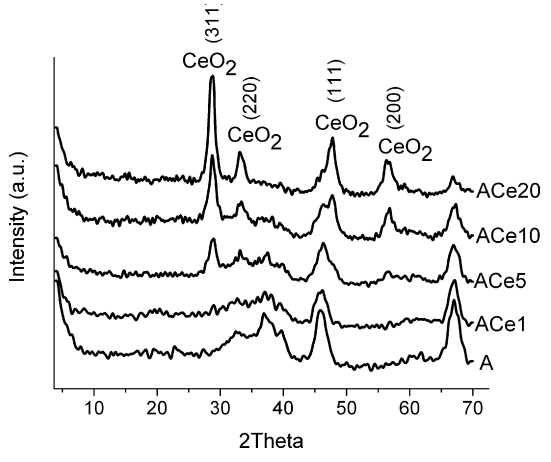

Fig. 3. XRD patterns for the A, ACe1, ACe5, ACe10 and ACe20 catalysts.

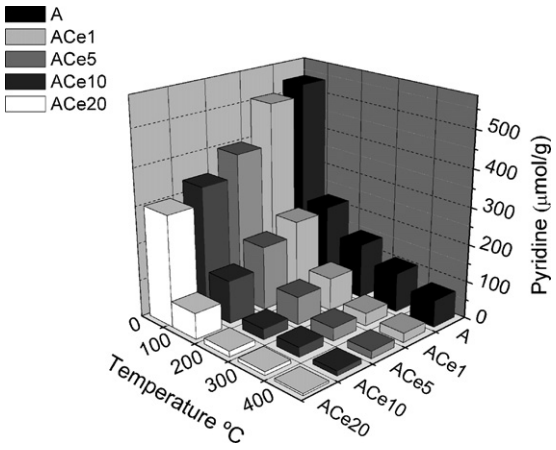

Fig. 4. Total acidity determined form the FTIR-pyridine absorption spectra in the A, ACe1, ACe5, ACe10 and ACe20 catalysts as a function of the cerium content and desorption temperature.

[14]. Stronger and well-defined CeO_2 reflections appeared at 20%Ce.

The acidic properties and nature of the sites generated in the ceria–alumina solids were determined by FTIR-pyridine adsorption as a function of the temperature [15]. The pyridine is adsorbed on the Brönsted and Lewis sites in the solid oxides [16]. The FTIR-pyridine spectra of the alumina doped supports showed absorption bands at 1590, 1490 and 1450 cm^{-1}, which have been assigned to pyridine adsorbed on the Lewis acid sites [17]. Brönsted acidity (1545 cm^{-1}) was not observed in any of the samples. The amount of adsorbed pyridine (μmol g^{-1}) as a function of the desorption temperature (25, 100, 200, 300, and 400 °C) for the various supports is shown in Fig. 4. A diminution of the total acid sites as a function of the Ce content was observed. Considering that the pyridine desorption temperature is an indirect measure of the strength of the acid sites, the catalysts with the strongest acid sites are those with the lowest cerium content.

The XPS cerium spectra for the ACe solids with various cerium contents are shown in Fig. 5. Several authors have reported the complexity of the Ce 3d spectra in ceria-based materials [18–20]. The binding energy Ce 3d of ACe1, ACe5, ACe10, and ACe20, for the characteristic Ce^{4+} component overlaps that corresponding to Ce^{3+}. However, the deconvolution of the spectra showed well-defined peaks that enabled the estimation of the relative contribution by the Ce^{4+} (CeO_2) and Ce^{3+} (Ce_2O_3) species (Table 1 and Fig. 5). The ACe1 sample presents two peaks in the $3d_{5/2}$ region corresponding to binding energies at around 881.5 and 885.2 eV which have been associated to Ce^{3+} [18,21]; and the band shape typical of Ce^{4+} at 898.0 eV and its corresponding energy for the $3d_{3/2}$ signal reported in Table 1. As for the ACe5, ACe10 and ACe20 samples, the $3d_{5/2}$ level energies around 885.5–885.8 eV assigned to Ce^{3+} as well as the peaks corresponding to the binding energies at 882.3–882.5 eV and 897.8–898.6 eV assigned to C^{4+} are observed [21]. The Ce^{4+} assignment is confirmed by the presence of the satellite structure at 914.0–916.5 eV (B.E. Ce $3d_{3/2}$ = 916 eV [22]), which is typical of tetravalent cerium species. The proportions of Ce^{4+}

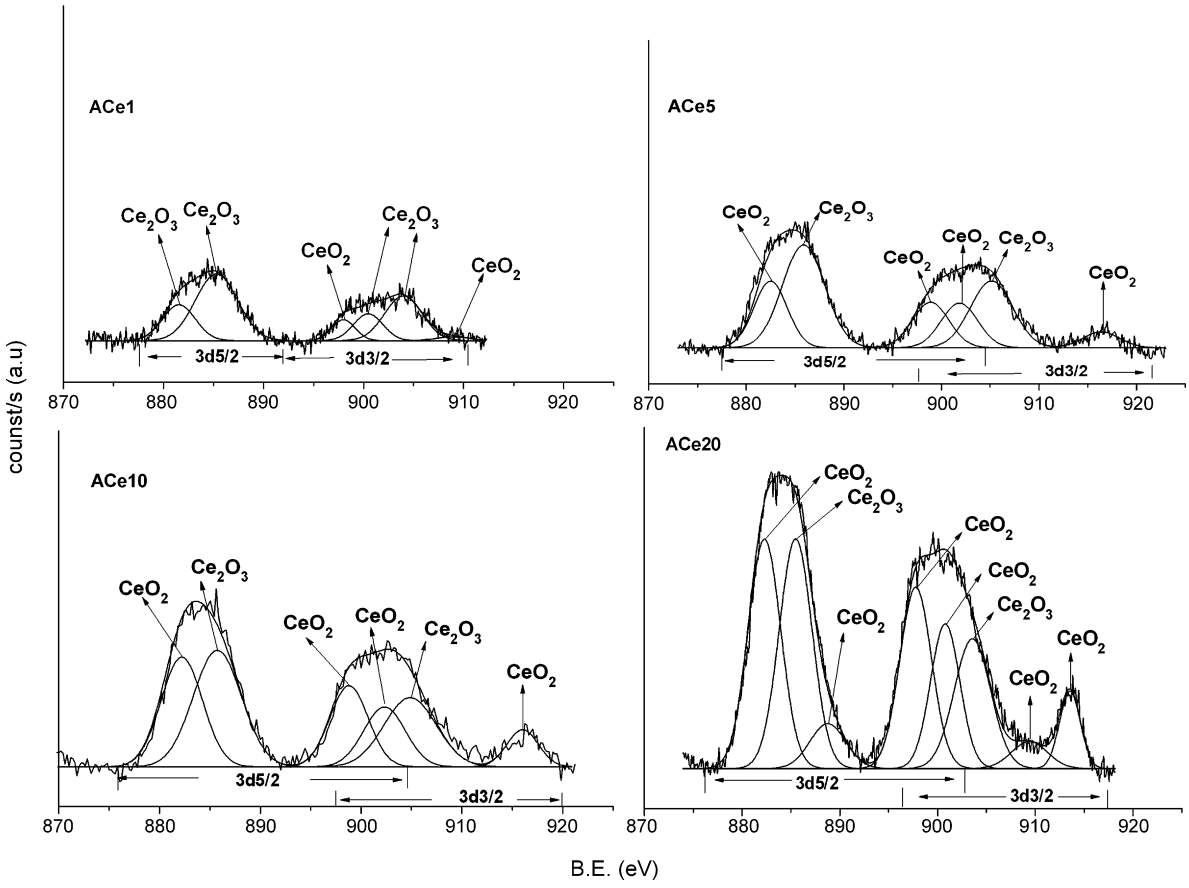

Fig. 5. XPS spectra of the Ce 3d region for the ACe1, ACe5, ACe10 and ACe20 catalysts.

and Ce^{3+} in the samples can be calculated from the areas of the relevant peak in the Ce 3d region [23,24] and the estimated values are reported in Table 1. The proportion of Ce^{3+} diminishes as the Ce content in the solid increases. We assume that at low ceria content, the Ce_2O_3 is stabilized on the acid sites of the alumina. As the loading of cerium oxide increases, it is more probable to find CeO_2, since is not directly in contact with the alumina, which was detected by XPS.

Table 1
Binding energy values (eV) for the Ce species in the samples calcined at 650 °C

Catalyst	Species	$Ce_{5/2}$ (eV)	$Ce_{3/2}$ (eV)	Ce^{4+}/Ce^{3+} [a]
ACe1–Ce3d	Ce^{3+}	881.5	900.7	0.14
	Ce^{3+}	885.2	903.8	
	Ce^{4+}	898.0	909.27	
ACe5–Ce3d	Ce^{4+}	882.5	901.8	0.8
	Ce^{3+}	885.8	904.7	
	Ce^{4+}	898.7	916.5	
ACe10–Ce3d	Ce^{4+}	882.3	901.3	1.2
	Ce^{3+}	885.5	904.6	
	Ce^{4+}	898.6	916.1	
ACe20–Ce3d	Ce^{4+}	882.3	900.8	2.1
	Ce^{3+}	885.5	903.5	
	Ce^{4+}	888.7	909.5	
	Ce^{4+}	897.8	914.0	

[a] Corresponding to CeO_2 (Ce^{4+}) and Ce_2O_3 (Ce^{3+}).

The atomic surface relationships between the different elements determined by XPS are reported in Table 2. The Al/O atomic surface ratio is almost constant for all the samples; whereas, the Ce/Al and Ce/O ratios increase with the cerium loading; these data imply that Ce is on the alumina surface.

The catalytic activity of the Al_2O_3–Ce solids toward the total oxidation of toluene is shown in Fig. 6. The catalytic behavior is described by a "S-Shape" light-off curve. The measurements of activity were carried out from 100 up to 400 °C. Two behaviors can be observed for the different solids. Firstly, the A and ACe1 samples, showed a very similar curve shape behavior. In these samples, no catalytic activity is observed from 100 to 270–275 °C; afterwards, a sudden increase in the combustion activity was observed by reaching total oxidation of toluene at temperatures of 379 and 358 °C for A an ACe1, respectively (Table 3). Secondly, as for the samples containing 5, 10 and 20 wt% Ce, the range of combustion tem-

Table 2
Selected XPS atomic ratios for the samples calcined at 650 °C

Label	Al/O	Ce/Al	Ce/O
A	0.65	–	–
ACe1	0.65	0.0036	0.0023
ACe5	0.66	0.0191	0.0125
ACe10	0.64	0.0339	0.0218
ACe20	0.66	0.0556	0.0349

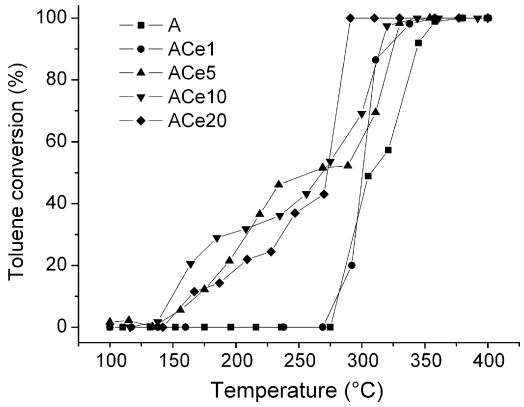

Fig. 6. Light off toluene combustion curves for the A, ACe1, ACe5, ACe10 and ACe20 catalysts.

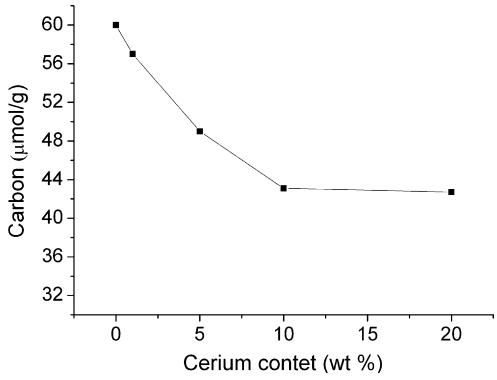

Fig. 7. Carbon deposited after 20 h of reaction as a function of the cerium content on the supports.

perature is higher; the combustion initiated at around 140 °C and reached 100% of toluene total conversion at 354, 343 and 290 °C, respectively. The effect of the Ce content on the toluene combustion is evident since the displacement to a lower temperature for the total combustion of toluene is of 89 °C for the Ce (20%) support in comparison with the reference alumina catalyst.

In the naphthalene combustion over a CeO_2 support with two different surface areas, it has been reported that the surface area and the strength of the bond between the adsorbed molecules and the catalyst surface were important parameters affecting the naphthalene catalytic combustion [6]. In the present case, the reaction rate expressed as mol m^{-2} s^{-1} and determined at 300 °C (Table 3), showed that the highest activity was shown by the catalysts with the lowest specific surface area. The specific combustion rate for 20% Ce solid loading (8.2×10^{-8} mol m^{-2} s^{-1} for 128 m^2 g^{-1}) is 3.6 higher than that showed by the Al_2O_3 (2.5×10^{-8} mol m^{-2} s^{-1} for 174 m^2 g^{-1}), according to these results, we can say that the surface area is not the responsible factor of the high activity in the ACeX catalysts.

The ability of cerium oxide to transport oxygen in combination with the redox cycle $Ce^{4+} \Leftrightarrow Ce^{3+}$can be related to the improvement in the toluene combustion. The XPS analysis showed the presence of the Ce^{3+} and Ce^{4+} species and their relative abundance; the Ce^{4+} increases with the Ce content in the sample. As for the ACe5, ACe10 and ACe20 solids, the Ce^{4+}/Ce^{3+} ratio was 0.8, 1.2 and 2.1, respectively. The sample with the lowest Ce^{4+}/Ce^{3+} ratio (0.14) is the less active among the ACeX samples. The trend of the Ce^{4+}/Ce^{3+} ratio follows the order ACe20 > ACe10 > ACe5 > ACe1 which is the same trend of the combustion activity at 300°. We assume, then, that the redox cycle $Ce^{4+} \Leftrightarrow Ce^{3+}$ is the main factor that improves the catalytic combustion activity. The correlation of the XPS concerning the fresh species can be assumed as an indirect determination to explain the overall reactions occurring in the reaction media: Ce^{4+} + toluene $\Leftrightarrow$ $Ce^{3+} + CO_2 + H_2O$, fast reaction; Ce^{3+} + oxygen $\Leftrightarrow$ $Ce^{4+} + H_2O$, slow reaction.

Table 3
Comparison of the catalytic activity expressed as T_{100} (°C) as function of the Ce loading and reaction rate at 300 °C

Catalyst	$T_{100\%\ C}$ (°C)[a]	Specific reaction rate (mol m^{-2} s^{-1} × 10^8)
γ-Al_2O_3	379	2.5
γ-Al_2O_3–Ce1	358	3.0
γ-Al_2O_3–Ce5	354	4.1
γ-Al_2O_3–Ce10	343	4.7
γ-Al_2O_3–Ce20	290	8.2

[a] Temperature for 100% combustion.

It is well known that in solids with high acidity, the deposit of carbon is a function of the acid strength; the deposit of carbon during combustion after 20 h of reaction was determined by TPO measurements. In Fig. 7 it is reported the amount of carbon deposited on the catalysts as a function of the cerium content; it follows the same order of the acidity on the catalysts; it is shown, i.e. the supports with the highest acidity are the catalysts with the highest amount of deposited carbon. As for the ACeX catalysts, with a higher Ce load, they showed the lowest formation of carbon during the toluene combustion which is due to two reasons, the presence of the lowest acid site strength and the role of cerium oxide as an oxygen source in the combustion of the carbon deposited on the catalysts.

4. Conclusions

In conclusion, the addition of cerium nitrate to boehmite leads to a diminution of the specific surface area on the γ-Al_2O_3–Ce catalysts. A decrease in the Lewis acidity occurred in the catalysts with the highest cerium oxide content. The XPS spectroscopy study revealed the presence of the Ce^{3+} and Ce^{4+} species; the aforementioned occurred in a higher proportion in the samples with the highest Ce content. The toluene combustion temperature is diminished as the cerium oxide content in the catalysts increases. It is showed that combustion activity can be correlated to the Ce^{4+}/Ce^{3+} ratio in the catalysts; the higher the Ce^{4+} proportion in the catalysts is the higher the combustion activity. It has been shown that the Al_2O_3–CeO_2 oxides are relevant catalysts for the VOC combustion.

Acknowledgements

We acknowledge CONACYT for their financial support of the research projects SEP-CONACYT-2004-C01-46689Q. J.M.

Padilla and I. Cuauhtémoc thank CONACYT for the grants awarded to them.

References

[1] V. Blaisin-Aubè, J. Belkouch, L. Monceaux, Appl. Catal. B: Environ. 43 (2003) 175–186.
[2] C. Lahousse, A. Bernier, P. Grange, B. Delmon, P. Papaefthimiou, T. Ionnides, X. Verykios, J. Catal. 178 (1998) 214–225.
[3] G. Pecchi, P. Reyes, R. Gòmez, T. Lòpez, J.L. Fierro, Appl. Catal. B: Environ. 17 (1998) L7–L13.
[4] B. de Rivas, J.I. Gutierrez-Ortiz, R. Lòpez-Fonseca, J.R. Gonzalez Velazco, Appl. Catal. A: Gen. 314 (2006) 54–63.
[5] M.F. Luo, M. He, Y.L. Xie, P. Fang, L.Y. Jin, Appl. Catal. B: Environ. 69 (2006) 213–218.
[6] T. Garcìa, B. Solsona, S.H. Taylor, Appl. Catal. B: Environ. 66 (2006) 92–99.
[7] S. Cimino, S. Colonna, S. De la Rossi, M. Faticanti, L. Lisi, H. Pettiti, P. Porta, J. Catal. 205 (2002) 309–317.
[8] M. Alfanti, M. Florea, S. Somacescu, V.I. Parvulescu, Appl. Catal. B: Environ. 60 (2005) 33–39.
[9] Trovarelli F., Catal. Rev. 38 (1996) 439–520.
[10] B. Levosseur, B. Renard, J. Barbier Jr., D. Duprez, React. Kinet. Catal. Lett. 87 (2006) 269–279.
[11] M. Meng, Y. Zha, J. Luo, T. Hu, Y. Xie, T. Liu, J. Zhang, Appl. Catal. A: Gen. 301 (2006) 145–151.
[12] R.J. Farrauto, R.M. Heck, Catal. Today 51 (1999) 351–360.
[13] T.R. Baldwin, R. Burch, Appl. Catal. 66 (1990) 359–381.
[14] D. Müller, W. Gessner, H.J. Behrens, G. Scheler, Chem. Phys. Lett. 79 (1981) 59–66.
[15] F.R. Chen, J.G. Davis, J.J. Fripiat, J. Catal. 133 (1992) 263–278.
[16] S. Rajagopal, T.L. Grim, D.J. Collins, R. Miranda, J. Catal. 137 (1992) 453–461.
[17] A. Wang, X. Bokhimi, O. Novaro, T. López, F. Tzompanzi, R. Gómez, J. Navarrete, M.E. Llanos, E. López-Salinas, J. Mol. Catal. A 137 (1999) 239–252.
[18] P. Burroughs, A. Hammett, A.F. Orchard, G. Thornton, J. Chem. Soc., Dalton Trans. 17 (1976) 1686–1698.
[19] G. Liu, J.A. Rodriguez, J. Hrbek, J. Dvorak, J. Phys. Chem. B. 105 (2001) 7762–7770.
[20] C. Larese, F. Cabello Galisteo, M. Lopez Granados, R. Mariscal, J.L.G. Fierro, P.S. Lambrou, A.M. Efstathiou, J. Catal. 226 (2004) 443–456.
[21] A. Pfau, K.D. Schierbaum, Surf. Sci. 321 (1994) 71–80.
[22] M.I. Zaki, G.A.M. Hussein, S.A.A. Manssur, H.M. Ismael, G.A.H. Merhemer, Colloid. Surf. A. 127 (1997) 47–52.
[23] J.Z. Shyu, W.H. Weber, H.S. Gandhi, J. Phys. Chem. 92 (1988) 4964–4970.
[24] X. Wu, L. Xu, D. Weng, Appl. Surf. Sci. 221 (2004) 375–383.